Inorganic Chemistry

Article

pubs.acs.org/IC

Oxyhydrides of (Ca,Sr,Ba)TiO_3 Perovskite Solid Solutions

Tatsunori Sakaguchi,[†] Yoji Kobayashi,[†] Takeshi Yajima,[†] Masatoshi Ohkura,[†] Cédric Tassel,[†,‡] Fumitaka Takeiri,[†] Shingo Mitsuoka,[†] Hiroshi Ohkubo,[†] Takafumi Yamamoto,[†] Jung eun Kim,[§] Naruki Tsuji,[§] Akihiko Fujihara,[§] Yoshitaka Matsushita,[∥] James Hester,[⊥] Maxim Avdeev,[⊥] Kenji Ohoyama,[#] and Hiroshi Kageyama*[,†]

[†]Department of Energy and Hydrocarbon Chemistry, Graduate School of Engineering, Kyoto University, Nishikyo-ku, Kyoto 615-8510, Japan

[‡]The Hakubi Center for Advanced Research, Kyoto University, Yoshida Ushinomiya-cho, Sakyo-ku, Kyoto 606-8302, Japan

[§]SPring-8/JASRI, 1-1-1 Kouto, Sayo-cho, Sayo-gun, Hyogo 679-5198, Japan

[∥]NIMS Beamline Station at SPring-8, National Institute for Materials Science, 1-1-1 Kouto, Sayo-cho, Sayo-gun, Hyogo 679-5148, Japan

[⊥]Bragg Institute, Australian Nuclear Science and Technology Organisation, PMB 1, Menai, NSW 2234, Australia

[#]Institute for Materials Research, Tohoku University, Sendai 980-8577, Japan

Supporting Information

ABSTRACT: The oxyhydride solid solutions (Ca,Sr)$TiO_{3-x}H_x$ and (Sr,Ba)$TiO_{3-x}H_x$ have been prepared by reducing the corresponding $ATiO_3$ oxides with calcium hydride. Under the reaction conditions examined, a hydride content of x = 0.1−0.3 was obtained for all compositions. Compared to our previous result with $BaTiO_{3-x}H_x$, the larger particle size in this study (20−30 μm vs 170 nm) resulted in a somewhat lower hydride amount despite prolonged reaction times. We examined changes in cell volume, octahedral tilt angle, and site occupancy of different anion sites after conversion to oxyhydrides; it appears that these oxyhydrides fit the geometrical descriptions typical for regular ABO_3 perovskites quite well. The hydrogen release temperature, previously shown to be indicative of the hydride exchange temperature, however, does not scale linearly with the A-site composition, indicating a potential effect of chemical randomness.

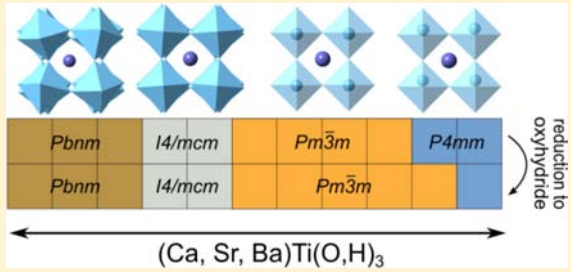

INTRODUCTION

We recently reported an oxyhydride of $BaTiO_3$, $BaTiO_{3-x}H_x$, with hydride substitution up to 20% (x = 0.6).[1] Such compounds, where oxide (O^{2-}) and hydride (H^-) ions occupy anionic sites, are still quite rare, especially for transition metals. Other than this, the transition metal oxyhydrides reported so far are $LaSrCoO_3H_{0.7}$ and $Sr_3Co_2O_{4.33}H_{0.84}$.[2,3] These compounds have been prepared by the topochemical reduction of parent oxides with calcium hydride in a solid state reaction. Although the two cobaltites are based on layered perovskites, $BaTiO_{3-x}H_x$ crystallizes in a simpler ABO_3 perovskite structure, and many systematic studies have been performed for this large family of titanium perovskites. In oxyhydrides, it appears that hydride ions are fairly mobile at relatively low temperatures (400 °C),[1,4] offering a unique opportunity to study the diffusion mechanism of hydride ions in oxide. Combined with the electric conductivity derived from Ti 3d electrons, there is much potential for material development as a mixed anionic/electronic conductor.

In $A^{2+}TiO_3$ perovskites, ferroelectric and dielectric properties vary as a function of temperature, pressure and A-site cation. Substitution at the A-site with the relatively small Ca forces the octahedra in the perovskite structure to adopt various tilted arrangements. Alternatively, substitution by other cations such as Pb or Bi can introduce superior dielectric properties via their lone pair electrons.[5,6] Such control of various properties with the A-site may also be possible with titanium oxyhydrides.

We recently expanded these oxyhydrides to thin films of $ATiO_{3-x}H_x$, with the alkali earths Ba, Sr, and Ca as the A-site cation.[7] In this paper, we have prepared the solid solutions $Sr_{1-x}Ba_xTi(O,H)_3$ and $Ca_xSr_{1-x}Ti(O,H)_3$, with hydride contents ranging from $ATiO_{2.9}H_{0.1}$ to $ATiO_{2.7}H_{0.3}$. We have carried out structural analysis using powder synchrotron X-ray and neutron diffraction to examine the effect of the hydridization reaction on lattice parameter and octahedral tilt. We have also examined the hydrogen release temperature under inert atmospheres, and found an unusual dependence on the A-site, indicating the capability of controlling deuteride/hydride exchange as well as mobility by adjusting the A site.

Received: April 26, 2012
Published: October 19, 2012

   dx.doi.org/10.1021/ic300859n | Inorg. Chem. 2012, 51, 11371−11376

EXPERIMENTAL SECTION

Preparation. Precursor $Sr_{1-x}Ba_xTiO_3$ and $Ca_xSr_{1-x}TiO_3$ (x = 0, 0.2, 0.4, 0.6, 0.8, 1.0) were synthesized by high temperature solid state reactions. Mixtures of $BaCO_3$ (99.99%, Rare Metallic), $SrCO_3$ (99.99%, Rare Metallic), $CaCO_3$ (99.99%, Rare Metallic), and TiO_2 (anatase, 99.99%, Rare Metallic) were weighed out in stoichiometric quantities, ground, pelletized, and preheated at 800 °C in air for half a day. Subsequently, the pellets were ground, repelletized and heated for 24 h at 1200 °C and 12 h at 1400 °C. Scanning electron microscopy (SEM) shows that the particles are around 20−30 μm in size. These resultant products and CaH_2 (99%, Aldrich) were mixed in a 1:3 molar ratio, ground, and pelletized in a N_2-filled glovebox (MBRAUN). The pellets were then sealed in an evacuated Pyrex tube with a residual pressure of less than 10^{-2} Pa. The sealed tubes were heated at 530 °C for 6−7 days. After the reaction, the products were ground in air and washed with a 0.1 M NH_4Cl/MeOH solution to remove excess CaH_2 and CaO.

Characterization. X-ray diffraction (XRD) patterns were collected at room temperature by a Bruker D8 Advance diffractometer equipped with a Cu K_α source (λ = 1.5406 Å). The synchrotron XRD experiments were performed at room temperature using a Debye−Scherrer camera installed at BL02B2 (λ = 0.774 Å) and BL15XU (λ = 0.342 Å) at SPring-8. Powder neutron diffraction experiments on the final products were carried out at room temperature on the Kinken powder diffractometer (λ = 1.850(4) Å, 331 Ge monochromator, 12′-blank-sample-18′/22′ collimation) "High Efficiency and High Resolution Measurements with multicounters" (HERMES), of the Institute for Materials Research (IMR), Tohoku University,[8] installed at the guide hall of the JRR-3 reactor in the Japan Atomic Energy Agency (JAEA), Tokai, Japan, and at Echidna (λ = 1.6220(8) Å, 335 Ge monochromator),[9] the Australian Nuclear Science and Technology Organisation (ANSTO), Australia. The synchrotron XRD and neutron data were analyzed by the LeBail/Rietveld method by the EXPGUI/GSAS[10,11] and Jana2006[12] programs. Thermal gravimetric analysis (TGA) was conducted with a Rigaku Thermo plus (TG 8120) using a Pt pan under flowing O_2 (300 mL/min). Hydrogen release was monitored by a Bruker MS9610 quadrupole mass spectrometer connected to this TGA instrument with an Ar flow of 300 mL/min.

RESULTS AND DISCUSSION

Changes in Symmetry. Eleven compositions, namely, $Ca_xSr_{1-x}TiO_3$ (x = 0, 0.2, 0.4, 0.6, 0.8, 1.0) and $Sr_{1-x}Ba_xTiO_3$ (x = 0.2, 0.4, 0.6, 0.8, 1.0) were prepared as parent compounds before treatment with calcium hydride. Because of the differing sizes of A-site cation, octahedral tilt and distortion results in a range of space groups (Figure 1a). $CaTiO_3$, $Ca_{0.2}Sr_{0.8}TiO_3$, and $Ca_{0.6}Sr_{0.4}TiO_3$ adopted the $GdFeO_3$-type (*Pbnm*) structure[13] (*Pnma* is the standard setting but we use *Pbnm* to keep all cell axes consistent across the A-site composition range). This structure has three tilt axes, which can be represented as $a^-a^-c^+$ in Glazer's notation,[14] and the unit cell is larger than the original primitive cell by $\sqrt{2}a_p \times \sqrt{2}a_p \times 2c_p$. Two anionic sites, O1 and O2, exist at the 4*c* and 8*d* Wyckoff positions. The next two compositions toward strontium ($Ca_{0.4}Sr_{0.6}TiO_3$ and $Ca_{0.2}Sr_{0.8}TiO_3$) adopted the tetragonal *I*4/*mcm* space group,[15] which is a one-tilt system ($a^0a^0c^-$) and also forms the same extended unit cell with two anionic sites O1 and O2 (4*a* and 8*h*). Some studies report the observation of a *Cmcm* phase within the Ca−Sr solutions,[16] but we have not observed this phase in our synchrotron X-ray patterns at room temperature. Most (Sr,Ba)TiO_3 compositions adopted the cubic *Pm*$\bar{3}$*m* space group ($a_p \times a_p \times a_p$ unit cell), with only $Sr_{0.2}Ba_{0.8}TiO_3$ and $BaTiO_3$ adopting the tetragonal *P4mm* space group because of a ferroelectric distortion, where the Ti cation is slightly displaced along the *c* axis from the octahedral center by approximately 0.08 Å.[17]

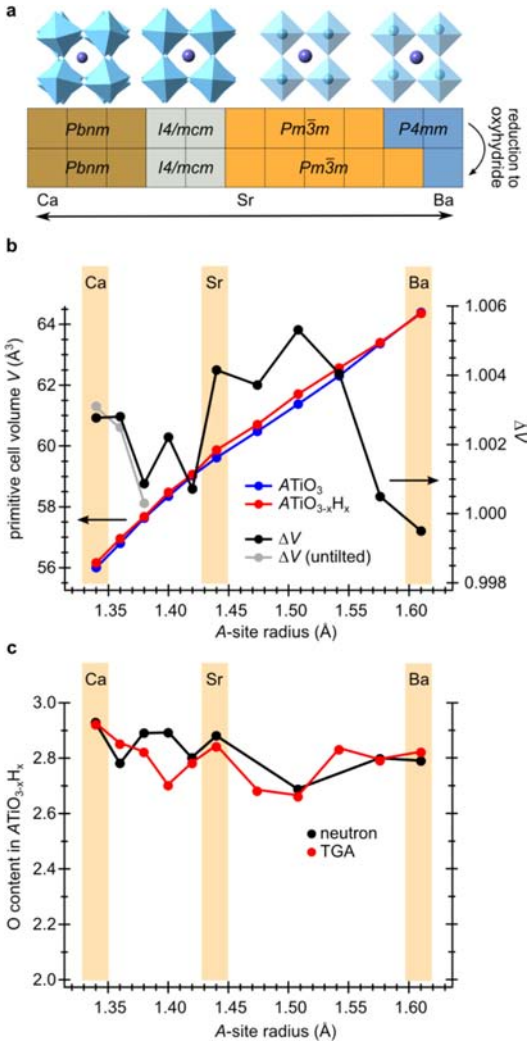

Figure 1. (a) Room temperature structures of $ATiO_3$ and $ATiO_{3-x}H_x$, all differing in tilt schemes or Ti displacement (the latter being exaggerated for *P4mm*). (b) Primitive cell volumes of parent oxides and oxyhydrides plotted in blue and red, respectively, together with the relative volume change ΔV (black/gray). Panel c compares the oxygen contents. For all plots, error bars fit within the markers when plotted.

In our previous study with $BaTiO_{3-x}H_x$, during conversion of the oxide to oxyhydride, we observed a symmetry change from the tetragonal *P4mm* space group to the cubic *Pm*$\bar{3}$*m* space group.[1] In this study, $BaTiO_{3-x}H_x$ is still tetragonal, although significantly close to being cubic (a = 4.0318(1) Å, c = 4.0402(3) Å). This may be due to the difference in particle size (170 nm in the previous study, vs 10−30 μm here, see Figure S1 in the Supporting Information), which results in slower reactivity and consequently smaller hydride concentration, as discussed again later. $Sr_{0.2}Ba_{0.8}TiO_3$ became cubic upon reduction. For the other tetragonal and orthorhombic phases of the Ca−Sr compositions, no change was observed; the XRD patterns were are all adequately fit with the same space group as the parent compound. These changes have also been summarized in Figure 1a. We note that at 530 °C (where the hydride reaction is performed), $BaTiO_3$ becomes cubic (*Pm*$\bar{3}$*m*),[18] while $CaTiO_3$ should remain orthorhombic (*Pbnm*).[19] In any event, the reason for the symmetry change upon reduction in only the Ba-rich region as opposed to the

dx.doi.org/10.1021/ic300859n | Inorg. Chem. 2012, 51, 11371−11376

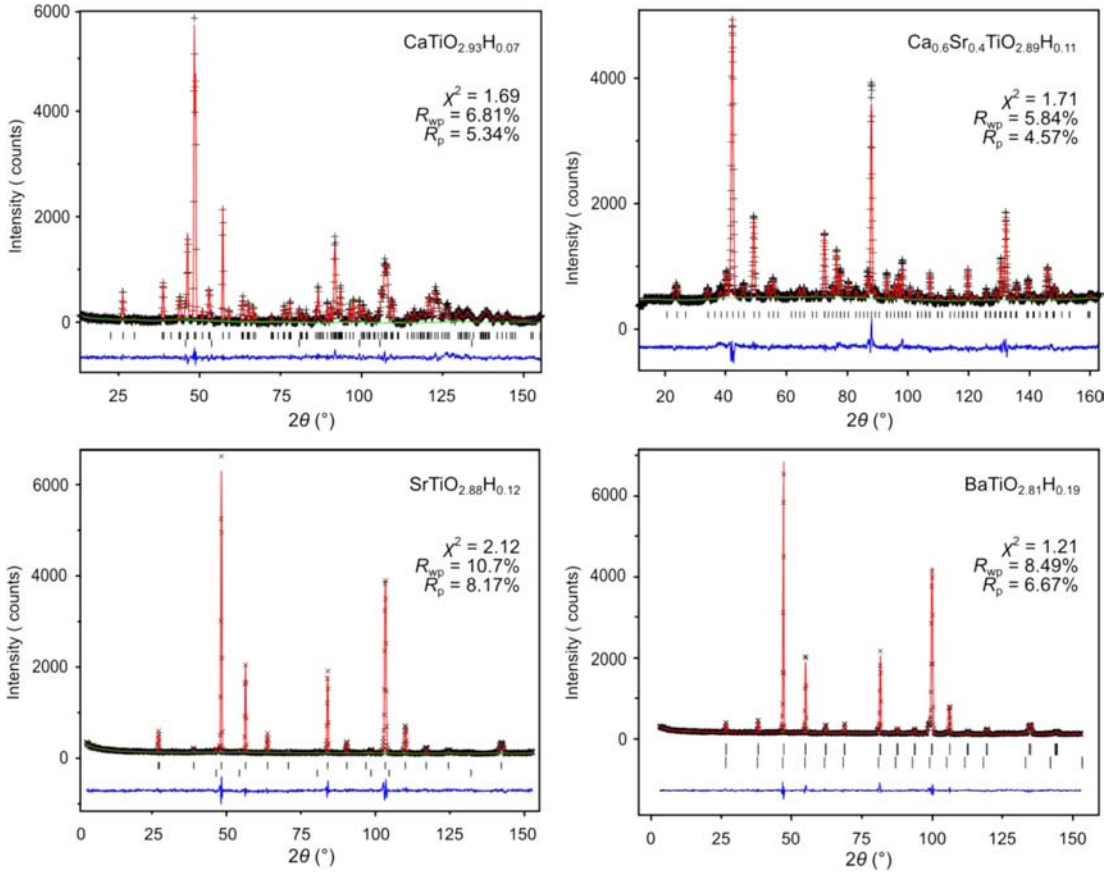

Figure 2. Rietveld refinements of neutron diffraction data of selected oxyhydride compositions. For $CaTiO_{2.84}H_{0.16}$ and $SrTiO_{2.82}H_{0.12}$, the second phase is from aluminum parts of the measurement cell. The second phase in $BaTiO_{2.79}H_{0.11}$ (lower right) is a minority phase with a larger lattice parameter (i.e., more reduced). In all refinements, the lattice parameters were fixed to those obtained from synchrotron X-ray data. The neutron wavelength for $Ca_{0.6}Sr_{0.4}TiO_{2.88}H_{0.12}$ is 1.6220(8) Å (Echidna, ANSTO), while for the other compositions the wavelength is 1.850(4) Å (HERMES, Tohoku Univ./JAEA).

Ca-rich region is that the original tetragonal space group is due to a ferroelectric distortion, rather than octahedral tilting. During treatment with CaH_2, reduction of the d^0 Ti center (i.e., electron doping to the Ti 3d t_{2g} subbands) removes this distortion, thus resulting in the cubic ideal structure.

In the orthorhombic compositions rich in calcium, the octahedrally coordinated titanium ions are already in a rather ideal geometry, so no change in the crystal symmetry is observed from the effect mentioned above. The deviation from the ideal cubic perovskite is instead determined by the octahedral tilt, which in turn can be explained by the small Ca^{2+} resulting in a small tolerance factor. The tolerance factor t is defined in equation 1 below:

$$t = \frac{R_X + R_A}{\sqrt{2}(R_X + R_B)} \quad (1)$$

where R_A is the A-site cation radius, R_B is the B-site cation radius, and R_X is the anion radius. The O^{2-} and H^- ions differ slightly in size (1.38 vs 1.54 Å),[20,21] but the exchange does not cause a large change to the tilt scheme. This is because the anionic radius R_X appears in both the numerator and denominator of equation 1. For example, let us examine the tolerance factor of $CaTiO_3$ after its change to the oxyhydride. Using typical ionic radii,[20] the tolerance factor t for $CaTiO_3$ is 0.869. Assuming a composition of $CaTiO_{2.8}H_{0.2}$ and averaged ionic radii (for O^{2-}/H^- and Ti^{4+}/Ti^{3+}), this value changes only slightly to 0.863, and even at $CaTiO_2H$, t = 0.838. Thus, conversion to oxyhydride may slightly increase the tilt angles, but should not adversely affect the entire tilt scheme, and our observations of the *Pbnm* space group in the product are justified. On a separate note, we have also conducted synchrotron XRD measurements of the oxyhydrides down to 90 K, and have not observed any structural phase transformations.

Changes in Cell Volume. The unit cell volumes (based on the reduced primitive cell) of the various compositions are plotted in Figure 1b. Here, for both parent oxides and oxyhydrides, the lattice parameters were taken from LeBail refinements of synchrotron XRD data; the error bars are generally within the size of the markers on the plot. In the parent oxide (blue line, Figure 1b), we see slight changes in slope for each space group throughout the composition range. Overall, the oxyhydride products show an expansion in cell volume (red and black lines, Figure 1b). In our previous report with $BaTiO_{3-x}H_x$,[1] we also observed this general trend of increasing cell volume with hydride content. Other than the anion size difference, the cell increase during reduction is in accordance with the larger size of Ti^{3+} over Ti^{4+} and longer, weaker Ti-anion bond lengths. Near the terminal composition $BaTiO_{3-x}H_x$, we see no change in cell volume, but this may be due to a gradual removal of the ferroelectric distortion compensating the cell expansion effect upon reduction, combined with the relatively low amount of hydride incorporation. The cubic Sr−Ba region shows the largest

dx.doi.org/10.1021/ic300859n | *Inorg. Chem.* 2012, 51, 11371−11376

Table 1. Crystallographic Data of (Ca,Sr)TiO_{3-x} H_x and $BaTiO_{3-x}H_x$[a]

$CaTiO_{2.93}H_{0.07}$[b]

atom	site	x	y	z	occ.	$100U_{iso}$
Ca	4c	−0.0093(9)	0.0352(6)	0.25	1	0.52(9)
Ti	4b	0	0.5	0	1	0.28(10)
O1	4c	0.0710(6)	0.4858(5)	0.25	0.976(5)	0.55(5)
O2	8d	0.7097(4)	0.2901(4)	0.0365(30)	0.976(5)	0.55(5)
H1	4c	0.0710(6)	0.4858(5)	0.25	0.024(5)	0.55(5)
H2	8d	0.7097(4)	0.2901(4)	0.0365(30)	0.024(5)	0.55(5)

$Ca_{0.4}Sr_{0.6}TiO_{2.89}H_{0.11}$[c]

atom	site	x	y	z	occ.	$100U_{iso}$
Ca	4b	0	0.5	0.25	0.4	0.64(9)
Sr	4b	0	0.5	0.25	0.6	0.64(9)
Ti	4c	0	0	0	1	0.03(12)
O1	4a	0	0	0.25	0.964(6)	1.75(7)
O2	8h	0.2246(3)	0.7246(3)	0	0.964(6)	1.75(7)
H1	4a	0	0	0.25	0.036(6)	1.75(7)
H2	8h	0.2246(3)	0.7246(3)	0	0.036(6)	1.75(7)

$Ca_{0.8}Sr_{0.2}TiO_{2.78}H_{0.22}$[d]

atom	site	x	y	z	occ.	$100U_{iso}$
Ca	4c	−0.007(2)	0.0252(8)	0.25	0.8	1.37(7)
Sr	4c	−0.007(2)	0.0252(8)	0.25	0.2	1.37(7)
Ti	4b	0	0.5	0	1	0.32(8)
O1	4c	0.064(1)	0.4866(8)	0.25	0.927(3)	0.68(5)
O2	8d	0.7152(5)	0.2847(5)	0.0309(4)	0.927(3)	0.68(5)
H1	4c	0.064(1)	0.4866(8)	0.25	0.073(3)	0.68(5)
H2	8d	0.7152(5)	0.2847(5)	0.0309(4)	0.073(3)	0.68(5)

$Ca_{0.2}Sr_{0.8}TiO_{2.80}H_{0.20}$[e]

atom	site	x	y	z	occ.	$100U_{iso}$
Ca	4b	0	0.5	0.25	0.2	1.3(1)
Sr	4b	0	0.5	0.25	0.8	1.3(1)
Ti	4c	0	0	0	1	0.128
O1	4a	0	0	0.25	0.932(6)	1.26(8)
O2	8h	0.2387(5)	0.7387(5)	0	0.932(6)	1.26(8)
H1	4a	0	0	0.25	0.068(6)	1.26(8)
H2	8h	0.2387(5)	0.7387(5)	0	0.068(6)	1.26(8)

$Ca_{0.6}Sr_{0.4}TiO_{2.89}H_{0.11}$[f]

atom	site	x	y	z	occ.	$100U_{iso}$
Ca	4c	−0.007(2)	0.168(8)	0.25	0.6	1.37(6)
Sr	4c	−0.007(2)	0.168(8)	0.25	0.4	1.37(6)
Ti	4b	0	0.5	0	1	1.00(6)
O1	4c	0.055(1)	0.495(1)	0.25	0.965(4)	1.49(3)
O2	8d	0.7225(7)	0.2778(7)	0.0244(4)	0.965(4)	1.49(3)
H1	4c	0.055(1)	0.495(1)	0.25	0.035(4)	1.49(3)
H2	8d	0.7225(7)	0.2778(7)	0.0244(4)	0.035(4)	1.49(3)

$BaTiO_{2.81}H_{0.19}$[g]

atom	site	x	y	z	occ.	$100U_{iso}$
Ba	1a	0	0	0	1	0.44(7)
Ti	1b	0.5	0.5	0.5	1	0.8(2)
O1	1b	0.5	0.5	0.0	0.9384(2)	0.42(2)
O2	2c	0.5	0	0.5	0.9384(2)	0.42(2)
H1	1b	0.5	0.5	0.0	0.0616(2)	0.42(2)
H2	2c	0.5	0	0.5	0.0616(2)	0.42(2)

[a]Numbers without errors in parentheses were fixed during the final refinement. [b]*Pbnm*, a = 5.38820(3) Å, b = 5.44716(3) Å, c = 7.65383(5) Å, χ^2 = 1.69, R_{wp} = 6.81%, R_p = 5.34%. [c]*I4/mcm*, a = 5.48347(4) Å, c = 7.77960(8) Å, χ^2 = 1.74, R_{wp} = 7.18%, R_p = 5.57%. [d]*Pbnm*, a = 5.42792(5) Å, b = 5.45549(5) Å, c = 7.69587(9) Å, χ^2 = 2.26, R_{wp} = 6.79%, R_p = 5.05%. [e]*I4/mcm*, a = 5.50506(4) Å, c = 7.7972(1) Å, χ^2 = 1.97, R_{wp} = 7.88%, R_p = 6.22%. [f]*Pbnm*, a = 5.47021(6) Å, b = 5.46110(6) Å, c = 7.72283(1) Å, χ^2 = 1.71, R_{wp} = 5.84%, R_p = 4.57%. [g]*P4mm*, a = 4.0318(1) Å, c = 4.0402(3) Å, χ^2 = 1.21, R_{wp} =8.49%, R_p = 6.67%; also containing a minority phase (12%), *Pm*$\bar{3}$*m*, a = 4.06 Å.

Table 2. Crystallographic Data of (Sr,Ba)$TiO_{3-x}H_x$ (*Pm*$\bar{3}$*m*)

composition	a (Å)	occ. O	occ. H	$100U_{iso}$ A	$100U_{iso}$ Ti	$100U_{iso}$ O/H	χ^2	R_{wp} (%)	R_p (%)
$SrTiO_{2.88}H_{0.12}$	3.91119(4)	0.960(6)	0.040(6)	0.9(1)	0.14	0.83(8)	2.12	10.7	8.17
$Sr_{0.6}Ba_{0.4}TiO_{2.71}H_{0.29}$	3.95164(7)	0.902(4)	0.098(4)	0.69(9)	1.1(1)	0.87(6)	1.57	9.33	7.20
$Sr_{0.2}Ba_{0.8}TiO_{2.80}H_{0.20}$[a]	3.98739(4)	0.935(3)	0.065(3)	0.68(6)	0.84(9)	0.76(4)	2.18	7.05	5.39

[a]Also containing a minority phase (10%), a = 4.09 Å.

volume increase, since no symmetry change is involved. On the other hand, in the Ca−Sr region, variable octahedral tilt may be somehow decreasing the apparent volume change, but we examine this in further detail later.

Rietveld Refinements. We also performed Rietveld refinements on the parent oxides (synchrotron XRD) and oxyhydride products (neutron diffraction). Peak profiles of the reduced samples showed that the relatively large particles resulted in slight inhomogeneities in anionic composition, presumably with a highly reduced minority (surface or small particles) and less-reduced majority phase (grain interior or large particles). This effect was especially visible in the Ba−Sr compositions and with the synchrotron XRD data because of the inherent high angular resolution (see Figure S2, Supporting Information). While a stable LeBail refinement to obtain the lattice parameter of the majority component is possible, the resulting asymmetric peak profiles make a meaningful Rietveld refinement difficult. However, the neutron diffractometers employed have lower angular resolution (vs synchrotron), in effect averaging out the peak profile in most cases so it may be adequately fit with a single phase, representing an averaged total of the sample. Two-phase refinements were necessary only for the two compositions toward $BaTiO_{3-x}H_x$. Representative refinement patterns of the neutron data for the oxyhydrides are shown in Figure 2 and results for all neutron data refinements are shown in Tables 1 and 2.

As mentioned earlier, synchrotron X-ray data shows that it is safe to start the neutron refinement of the oxyhydrides based on the structures of the parent oxides, except for $Sr_{0.2}Ba_{0.8}Ti(O,H)_3$ where the $BaTiO_3$-structure type (*P4mm* space group) is used. Oxide and hydride were randomly distributed at the anionic site(s) of each structural model. In addition, we set the occupancies of the anionic vacancies to zero; that is, constrained "O + H" to unity. In our previous study with $BaTiO_{3-x}H_x$,[1] we found that the amount of anionic vacancies are indeed very small, based on a combination of X-ray/

dx.doi.org/10.1021/ic300859n | *Inorg. Chem.* 2012, 51, 11371−11376

neutron Rietveld refinement, thermal gravimetric analysis, and magnetic measurements. By extension, we have assumed that the solid solutions in this paper also have very few anionic vacancies. This assumption enables us to use neutron diffraction data to adequately refine the anionic composition and atomic coordinates.

O^{2-}/H^{-} composition. The O^{2-}/H^{-} content based on refining the neutron data are shown by the black dots in Figure 1c. In the tetragonal and orthorhombic compositions, there are two anionic sites. During the refinement, the partial occupancies and thermal displacement factors of these two sites have been constrained to be equal to each other. In general, the composition ranges from $ATiO_{2.7}H_{0.3}$ to $ATiO_{2.9}H_{0.1}$ for all A-site compositions. The anion content of the oxyhydride samples can also be calculated from TGA under O_2 flow, as the oxyhydride reverts back to the parent oxide composition (representative data in Figure S3, Supporting Information). We see a general agreement in Figure 1c between the compositions obtained by neutron diffraction and TGA. Given the sensitivity of neutron diffraction to both oxide and hydride, this close agreement supports our approximation of assuming full anion occupancy. We do not see strong evidence for preferential hydride occupancy at either anionic site, and correlation effects also make it difficult to confirm. Such preferential occupancies are probably more pronounced in layered systems.

Octahedral Tilt. As previously mentioned, in the Ca–Sr region, octahedral tilt ($a^-a^-c^+$) is present. For example, in $CaTiO_3$, the octahedra at room temperature are each tilted at approximately 13° from the primitive crystallographic axis of the otherwise ideal cubic unit cell.[21] Based on the refined atomic coordinates in Tables 1 and 2, we determined the tilt angles in both the parent oxides and oxyhydrides, and plotted the results in Figure 3. Given the two anionic sites O1 and O2 in *Pbnm* and *I4/mcm*, two Ti–O–Ti bond angles are present. The Ti–O1–Ti angle reflects a mixture of the three tilt axes ($a^-a^-c^+$) in *Pbnm*, and becomes 180° in *I4/mcm*. The Ti–O2–Ti angle in the *I4/mcm* structure reflects only the c^- contribution of the $a^0a^0c^-$ scheme, and for the *Pbnm* structure there is an additional contribution from the other tilt axes. For our oxyhydride products, in general the observed tilt angles are within expected values for the given tilt system. In the *I4/mcm* region, it appears that conversion to oxyhydride influences the Ti–O2–Ti angle, especially in the *I4/mcm* region and this may be related to the tendency of increased hydride substitution at the O2 site seen in Figure 1c.

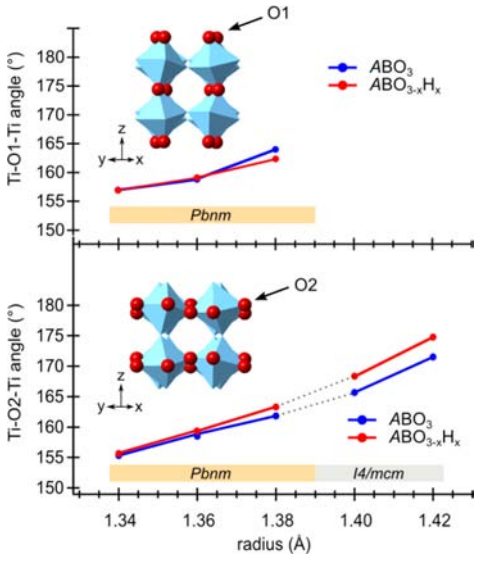

Figure 3. Angles between tilting octahedra before and after conversion to oxyhydride.

The octahedral tilt affects the total unit cell volume, and it is possible to recalculate the cell volume assuming this tilt is removed from the structure while preserving other structural aspects.[22−24] Doing so may explain some of the features in the Ca–Sr region of the ΔV curve in Figure 1b. We have conducted this analysis for the three-tilt region (i.e., *Pbnm* region) by calculating the tilt from the atomic coordinates, and then applying the following relationship, as done originally by O'Keefe[22] and later by Zhao et al.:[23,24]

$$V = abc = V_0 \cos^2 \Phi \quad (2)$$

Here, V is the cell volume found from the lattice parameters a, b, and c; V_0 is the volume of the untilted unit cell; and Φ is the tilt angle of the octahedra from the [111] direction, as defined by O'Keefe.[22] In Figure 1b, we compare two volume changes with the axis on the right-hand side. The black line (ΔV) represents the relative volume change due to hydridization, with cell volumes being calculated directly from the lattice parameters. The gray line (ΔV untilted) represents the same relative volume change upon reaction, but using idealized cell volumes for both the parent and oxyhydrides after applying eq 2. Comparison of these two results shows little deviation, so the effect on overall cell volume is rather small. In other words, the volume change brought by reduction is due to changes in ionic radii after all, rather than octahedral tilt.

H_2 Release temperature. When heated under inert atmospheres, $BaTiO_{3-x}H_x$ releases H_2 at 450 °C, and then scavenges residual oxygen to form a slightly reduced $BaTiO_{3-\delta}$ product. In hydrogen-containing atmospheres (such as D_2) close to or slightly below this temperature, hydride exchange occurs instead (i.e., resulting in $BaTiO_{3-x}H_yD_z$).[1] Hence, the H_2 release temperature of these $ATiO_{3-x}H_x$ oxyhydrides can be thought of as one indicator of when the hydride becomes mobile and exchangeable. Figure 4 shows thermal gravimetric analysis/mass spectrometry (TGA-MS) of the $ATiO_{3-x}H_x$ series. In general, hydrogen release peaks at 380–460 °C depending on the composition. Rather than exhibiting one peak, in some cases a broad background peak is observed (such as for $CaTiO_{2.81}H_{0.19}$, the top trace in Figure 4a). This may be related to inhomogeneities in the sample. In any event, when comparing the temperatures of the major peaks for each composition (plotted in Figure 4b), the pure Ca/Sr/Ba compositions seem to release hydrogen at significantly higher temperatures. This is rather curious as the particle sizes of the oxyhydrides (as observed by SEM; see Supporting Information Figure S1) are all about the same, and the hydride content for each sample does not show such a dependence on A-site composition. In A-site solid solutions of manganese perovskites, phase stability and magnetoresistivity scales with the variance of the distribution of the A-site cation size, or in other words, chemical disorder,[25−27] so perhaps this is a similar effect. In order to conclude this, a similar study using particles with a constant (and uniform) concentration of hydride ions is desired, which is in progress.

dx.doi.org/10.1021/ic300859n | *Inorg. Chem.* 2012, 51, 11371−11376

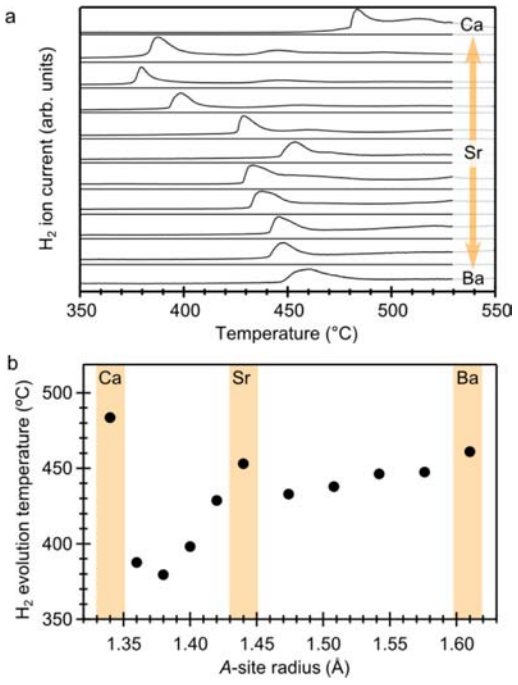

Figure 4. (a) shows H_2 gas evolution from various $ATiO_{3-x}H_x$ compositions during heating under flowing argon. From top to bottom, $Ca_xSr_{1-x}TiO_3$ (x = 0, 0.2, 0.4, 0.6, 0.8, 1.0) and $Sr_{1-x}Ba_xTiO_3$ (x = 0.2, 0.4, 0.6, 0.8, 1.0). The H_2 gas amount is monitored by a mass spectrometer. (b) Peak temperatures from a as a function of A-site cation radius.

CONCLUSION

We previously prepared the oxyhydride of $BaTiO_3$ and epitaxial films of $ATiO_{3-x}H_x$. Here, we have examined the structures of the solid solutions in detail. We note that the particle size used here was very large compared to our previously reported synthesis of $BaTiO_{2.4}H_{0.6}$ (30 μm vs 170 nm), and so with smaller particle sizes, higher hydride contents and facile deuteride exchange should be possible for these solid solutions. Despite the somewhat inhomogeneous nature of the samples, we find that the structural aspects of these $ABO_{3-x}H_x$ perovskites can be explained quite well in terms of the existing ABO_3 perovskites. Other A-site cations, such as Pb or vacancies ($La_{2/3}\square_{1/3}$) could also be possible, and we also hope to further expand the group of oxyhydrides to various layered and nonperovskite systems.

ASSOCIATED CONTENT

Supporting Information

Representative SEM images of $ATiO_3$ and $ATiO_{3-x}H_x$, X-ray/neutron diffraction profiles, representative TGA data, and lattice parameter trends. This material is available free of charge via the Internet at http://pubs.acs.org

AUTHOR INFORMATION

Corresponding Author

*E-mail: kage@scl.kyoto-u.ac.jp.

Notes

The authors declare no competing financial interest.

ACKNOWLEDGMENTS

This work was supported by the Japan Society for the Promotion of Science (JSPS) through its "Funding Program for World-Leading Innovative R&D on Science and Technology (FIRST) Program". The neutron experiment at Echidna (ANSTO) was supported by the Japanese Society for Neutron Science. T.Y. was supported by the Japan Society for the Promotion of Science for Young Scientists.

REFERENCES

(1) Kobayashi, Y.; Hernandez, O. J.; Sakaguchi, T.; Yajima, T.; Roisnel, T.; Tsujimoto, Y.; Morita, M.; Noda, Y.; Mogami, Y.; Kitada, A.; Ohkura, M.; Hosokawa, S.; Li, Z.; Hayashi, K.; Kusano, Y.; Kim, J. e.; Tsuji, N.; Fujiwara, A.; Matsushita, Y.; Yoshimura, K.; Takegoshi, K.; Inoue, M.; Takano, M.; Kageyama, H. *Nat. Mater.* **2012**, *11*, 507−511.
(2) Hayward, M. A.; Cussen, E. J.; Claridge, J. B.; Bieringer, M.; Rosseinsky, M. J.; Kiely, C. J.; Blundell, S. J.; Marshall, I. M.; Pratt, F. L. *Science* **2002**, *295*, 1882−1884.
(3) Helps, R. M.; Rees, N. H.; Hayward, M. A. *Inorg. Chem.* **2010**, *49*, 11062−11068.
(4) Bridges, C. A.; Fernandez-Alonso, F.; Goff, J. P.; Rosseinsky, M. J. *Adv. Mater.* **2006**, *18*, 3304−3308.
(5) Shirane, G.; Suzuki, K.; Takeda, A. *J. Phys. Soc. Jpn.* **1952**, *7*, 12−18.
(6) Buhrer, C. F. *J. Chem. Phys.* **1962**, *36*, 798−803.
(7) Yajima, T.; Kitada, A.; Kobayashi, Y.; Sakaguchi, T.; Bouilly, G.; Kasahara, S.; Terashima, T.; Takano, M.; Kageyama, H. *J. Am. Chem. Soc.* **2012**, *134*, 8782−8785.
(8) Ohoyama, K.; Kanouchi, T.; Nemoto, K.; Ohashi, M.; Kajitani, T.; Yamaguchi, Y. *Jpn. J. Appl. Phys.* **1998**, *37*, 3319−3326.
(9) Liss, K.-D.; Hunter, B. A.; Hagen, M. E.; Noakes, T. J.; Kennedy, S. J. *Phys. B* **2006**, *385*−*386*, 1013−1015.
(10) Toby, B. H. *J. Appl. Crystallogr.* **2001**, *34*, 210−213.
(11) Larson, A. C.; Von Dreele, R. B. *Los Alamos Natl. Lab., [Rep.] LA (U. S.)* **2004**, 86−748.
(12) Petricek, V.; Dusek, M.; Palatinus, L. *Jana2006. The Crystallographic Computing System*; Institute of Physics: Praha, Czech Republic, 2006.
(13) Kay, H. F.; Bailey, P. C. *Acta Crystallogr.* **1957**, *10*, 219−226.
(14) Glazer, A. M. *Acta Crystallogr.* **1972**, *B28*, 3384−3392.
(15) Yamanaka, T.; Hirai, N.; Komatsu, Y. *Am. Mineral.* **2002**, *87*, 1183−1189.
(16) Ball, C. J.; Begg, B. D.; Cookson, D. J.; Thorogood, G. J.; Vance, E. R. *J. Solid State Chem.* **1998**, *139*, 238−247.
(17) Kwei, G. H.; Lawson, A. C.; Billinge, S. J. L.; Cheong, S. W. *J. Phys. Chem.* **1993**, *97*, 2368−2377.
(18) Megaw, H. D. *Nature* **1945**, *155*, 484−485.
(19) Ali, R.; Yashima, M. *J. Solid State Chem.* **2005**, *178*, 2867−2872.
(20) Shannon, R. D.; Prewitt, C. T. *Acta Crystallogr.* **1969**, *B25*, 925−946.
(21) Ernslay, J. *The Elements*, 2nd ed.; Clarendon Press, Oxford, U.K., 1991.
(22) O'Keefe, M.; Hyde, B. G. *Acta Crystallogr. B* **1977**, *33*, 3802−3813.
(23) Zhao, Y.; Weidner, D. J.; Parise, J. B.; Cox, D. E. *Phys. Earth Planet. Inter.* **1993**, *76*, 1−16.
(24) Zhao, Y.; Weidner, D. J.; Parise, J. B.; Cox, D. E. *Phys. Earth Planet. Inter.* **1993**, *76*, 17−34.
(25) Rodríguez-Martínez, L. M.; Attfield, J. P. *Phys. Rev. B* **1996**, *54*, R15622−R15625.
(26) Rodríguez-Martínez, L. M.; Attfield, J. P. *Phys. Rev. B* **2000**, *63*, 024424/1−024424/7.
(27) Attfield, J. P. *Cryst. Eng.* **2002**, *5*, 427−438.